NIH Public Access
Author Manuscript
J Comp Physiol B. Author manuscript; available in PMC 2013 December 10.

Published in final edited form as:
J Comp Physiol B. 2009 July ; 179(5): . doi:10.1007/s00360-009-0339-3.

Lung respiratory rhythm and pattern generation in the bullfrog: role of neurokinin-1 and μ-opioid receptors

B. L. Davies, **C. M. Brundage**, **M. B. Harris**, and **B. E. Taylor**
Institute of Arctic Biology, University of Alaska Fairbanks, Rm 311 Irving I, 902 N Koyukuk Drive, Fairbanks, AK 99775, USA

B. E. Taylor: ffbet@uaf.edu

Abstract

Location of the lung respiratory rhythm generator (RRG) in the bullfrog brainstem was investigated by examining neurokinin-1 and μ-opioid receptor (NK1R, μOR) colocalization by immunohistochemistry and characterizing the role of these receptors in lung rhythm and episodic pattern generation. NK1R and μOR occurred in brainstems from all developmental stages. In juvenile bullfrogs a distinct area of colocalization was coincident with high-intensity fluorescent labeling of μOR; high-intensity labeling of μOR was not distinctly and consistently localized in tadpole brainstems. NK1R labeling intensity did not change with development. Similarity in colocalization is consistent with similarity in responses to substance P (SP, NK1R agonist) and DAMGO (μOR agonist) when bath applied to bullfrog brainstems of different developmental stages. In early stage tadpoles and juvenile bullfrogs, SP increased and DAMGO decreased lung burst frequency. In juvenile bullfrogs, SP increased lung burst frequency, episode frequency, but decreased number of lung bursts per episode and lung burst duration. In contrast, DAMGO decreased lung burst frequency and burst cycle frequency, episode frequency, and number of lung bursts per episode but increased all other lung burst parameters. Based on these results, we hypothesize that NK1R and μOR colocalization together with a metamorphosis-related increase in μOR intensity marks the location of the lung RRG but not necessarily the lung episodic pattern generator.

Keywords

Respiratory rhythmogenesis; Episodic breathing; Isolated brainstem

Introduction

Neural control of breathing has been most extensively investigated in mammals, which typically breathe in a pattern of continuous lung ventilation. Two distinct neuronal networks within the brainstem are proposed to be essential for respiratory rhythm generation in mammals (Onimaru et al. 1997; Rekling and Feldman 1998); inspiratory neurons in the preBötzinger complex (PBC; Smith et al. 1991; Gray et al. 2001) and pre-inspiratory neurons in the parafacial respiratory group (pFRG; Onimaru et al. 1995). Of these, the mammalian PBC has been proposed (Rekling and Feldman 1998) to be the kernel of respiration, but its primacy is called into question by the existence and identified function (Guyenet et al. 2005) of respiratory rhythm-generating pacemakers in the parafacial

© Springer-Verlag 2009

Correspondence to: B. E. Taylor, ffbet@uaf.edu.

Communicated by H. V. Carey.

NIH-PA Author Manuscript
NIH-PA Author Manuscript
NIH-PA Author Manuscript

NIH-PA Author Manuscript

NIH-PA Author Manuscript

NIH-PA Author Manuscript

respiratory group (pfRG). Given the proposed homology among vertebrate respiratory control networks, it would be useful to identify structural and functional commonalities in mammalian and amphibian respiratory control networks.

The PBC contains a high density of neurokinin-1 receptor-(NK1R) expressing neurons (Gray et al. 1999, 2001). These neurons are necessary for maintaining a normal respiratory rhythm (Gray et al. 2001; Wang et al. 2002). The PBC contains a large number of neurons expressing substance P (SP) (Liu et al. 2004), and local application of SP to the PBC increases respiratory frequency in rats (Gray et al. 1999). Mammalian PBC inspiratory neurons express μOR, and μ-opioids decrease respiratory frequency (Takeda et al. 2001). Colocalization of NK1R and μOR has been used to determine the location of the PBC, a respiratory rhythm generator (RRG) in mammalian brainstem slices (Gray et al. 1999).

Bullfrogs exhibit two distinct ventilatory motor patterns: rhythmic buccal and lung ventilation, with the latter often occurring in episodes (Kinkead and Milsom 1994). The rhythmic, episodic, bimodal pattern of breathing in bullfrogs is proposed to be the combined output of two RRG located in the brainstem, one for buccal and one for lung ventilation. An area essential for lung bursts is located between the auditory and glossopharyngeal nerves, and an area essential for buccal bursts but not lung bursts is located at the level of the vagus nerve (Wilson et al. 2002). The brainstem neurons that generate lung ventilation in the bullfrog are proposed to be homologous to those that generate breathing in mammals (Vasilakos et al. 2005; Wilson et al. 2006). In intact adult bullfrogs and isolated brainstems prepared from juveniles, μ-opiates depress lung burst frequency while buccal rhythm remains constant (Vasilakos et al. 2005) and SP increases lung burst frequency (Chen and Hedrick 2008). This similarity in roles of neuromodulators suggests parity between the mammalian PBC and the bullfrog lung RRG. The distribution of enkephalin, SP, and somatostatin is also similar in brainstems from frogs and mammals (Stuesse et al. 2001). Similarities in neuroanatomy and neurochemistry suggest that, bullfrog and mammalian breathing could be controlled by homologous or homoplastic neural networks.

Bullfrog episodic ventilation is characterized by lung activity occurring in a cluster of lung breaths separated from similar clusters by non-ventilatory activity and/or continuous buccal ventilation. This ventilatory pattern is multifarious; it can vary in the duration of episodes, the number of breaths occurring per episode and the duration of the non-ventilatory activity between episodes (Kinkead and Milsom 1994, 1996, 1997). Studies investigating the mechanisms underlying episodic breathing have looked at central and peripheral chemoreceptors (West et al. 1987; Smatresk and Smits 1991; Kinkead and Milsom 1994), pulmonary stretch receptors (Kinkead and Milsom 1996, 1997) and olfactory receptors (Kinkead and Milsom 1996). It was shown that each receptor group influenced breathing pattern by altering the number of breaths per episode, the duration of the non-ventilatory activity between episodes, or both. None of the receptor groups was shown to be directly responsible for episodic pattern generation (Kinkead 1997), and it was concluded that the mechanisms responsible for episodic pattern formation might be an intrinsic property of the central respiratory control network (Kinkead et al. 1994). Thus, the hypothesis of Jackson (1978), which proposes that episodes rather than individual breaths are the fundamental output of the respiratory control network has been supported and stands as a potential major difference between typical bullfrog and typical mammalian ventilation.

Identifying the mechanism of episodic pattern generation is complicated by the fact that changes in episode pattern may be the indirect result of changes rhythm generation and overall ventilatory drive. Studies with baclofen (Straus et al. 2000a, b) and neuronal nitric oxide synthase inhibitor (Harris et al. 2002) have shown that episodic pattern generation can

NIH-PA Author Manuscript

NIH-PA Author Manuscript

NIH-PA Author Manuscript

be altered independently from rhythm generation. The mechanism of episodic pattern formation, however, remains undetermined.

One aim of this study was to use double-label immunofluorescence techniques to identify colocalization of NK1R and μOR. We hypothesized that such colocalization would exist in the putative location of the bullfrog lung RRG implying similarity to the mammalian PBC. Immunofluorescence experiments were performed on bullfrogs of different developmental stages because the lung RRG exists throughout development, and we expected NK1R and μOR colocalization to exist throughout development. We repeated electrophysiological investigations of the role of NK1R and μOR in respiratory rhythm generation, which have been previously performed by Vasilakos et al. (2005) and Chen and Hedrick (2008), to add a consideration of the role of these receptors in episodic pattern generation. Determining the neural mechanisms responsible for episodic pattern generation has proven elusive. By investigating the role of NK1R and μOR in the generation of episodic pattern, we hoped to provide some insight in this matter.

Methods

Animals

Electrophysiology studies were performed on *Lithobates* (formerly *Rana) catesbeiana* juvenile bullfrogs (n = 12) and early stage tadpoles (n = 12) of either sex purchased from a commercial supplier (Sullivan, Nashville, TN, USA). All animals were maintained at 25°C in aquaria and were fed crickets (bullfrogs) or fish food (tadpoles). The institutional animal care and use committee (IACUC) approved the animal and research protocols. Experimental protocols adhered to local and national ethics standards.

Tadpoles and juvenile bullfrogs were used for immunofluorescence protocols to compare mean intensity and colocalization of NK1R and μOR among developmental stages. Classification of tadpoles was based on a grouping of the stages defined by Taylor and Köllros (1946, TK stages): early stage tadpoles were TK stages I–X (n = 6), middle-stage tadpoles were TK stages XI–XVII (n = 6), late-stage tadpoles were TK stages XVIII–;XXV (n = 6) and juvenile bullfrogs were TK stages XXV+ (n = 8).

Surgical preparation

Each animal was anesthetized by immersion for 1–2 min in a cold (4°C) 0.5% w/v solution of tricaine methanesulfonate (MS222, Sigma Chemical, St Louis, MO, USA) in dechlorinated water buffered with $NaHCO_3$ to pH 7.8. The dorsal cranium was removed and the forebrain rostral to the optic lobes was resected. The fourth ventricle was exposed by removing the choroid plexus. The brainstem and spinal cord were removed en bloc from the cranium and spinal canal. The dura mater was stripped, and the brain was transected rostral to the optic tectum and caudal to the brachial nerve. During the dissection, the brainstem was superfused with cold (4°C) artifical cerebrospinal fluid (aCSF) composed of (in mM) 104 NaCl, 4 KCl, 1.4 $MgCl_2$, 10 D-glucose, 25 $NaHCO_3$ and 2.4 $CaCl_2$.

Immunofluorescence

Brainstems (each an en bloc mass of tissue including the optic tectum, pons, medulla, cerebellum, and the anterior portion of the spinal cord) were isolated from eight juvenile bullfrogs and six early-, middle- and late-stage tadpoles according to the protocol described above (“Surgical preparation”). Brainstems were fixed in 4% paraformal-dehyde in PBS for 24 h and stored in 30% glucose until slicing. Brainstems were frozen in optimum cutting temperature (OCT) compound (Fischer, Pittsburgh, PA, USA), and mounted and cross-sectioned using an IEC Minitome cryostat (IEC, Needham Heights, MA, USA). Each brain-

NIH-PA Author Manuscript

NIH-PA Author Manuscript

NIH-PA Author Manuscript

stem was sectioned into about 200–400 16-μm thick slices, which were mounted on gelatin-coated slides and stored at −80°C until staining. Slides were washed three times for 10-min intervals in PBS composed of (in mM) 136.9 NaCl, 2.68 KCl, 10.4 Na_2HPO_4, and 1.8 KH_2PO_4. Slides were incubated for 2 h with blocker (3% Triton-X and 5% Donkey Serum in PBS) and for 48 h with the primary antibody solution at 4°C. The primary antibodies were mouse anti-NK1R receptor monoclonal antibody (1:20,000; Invitrogen Corp., Carlsbad, CA, USA) and rabbit anti-μOR polyclonal antibody (1:75,000; Immunostar, Hudson, WI, USA). Thus, we used mammalian antibodies to locate amphibian receptors, and we are compelled to add the caveat that in the absence of gene sequence data for these receptors in this species, the exact specificities of these antibodies for their target receptors are unknown. Slides were rinsed twice for 5 min and once for 1 h in PBS. Slides were incubated for 1 h with secondary antibody solution containing anti-mouse rhodamine red (RRX; 1:700; Jackson Immunoresearch, West Grove PA) and anti-rabbit fluoresceine (FitC, 1:500; Jackson Immunoresearch). Slides were rinsed with PBS six times for 5-min intervals and stored at 4°C to dry. Slides were hydrated with Vectashield (Vector Laboratories Inc., Burlingame, CA, USA) and cover slipped.

Slices were viewed using an Axioplan Imaging fluorescent microscope (Zeiss, Thornwood, NY, USA) equipped with Metamorph imaging software (Molecular Devices, Downington, PA, USA). Locations of regions of interest were determined using measurement and calibration options in Metamorph. The region of interest was identified by visually surveying staining results of 200–400 slices per brainstem. The region of interest is only the region of colocalization that was consistent in brainstems of all tadpole stages.

Images of whole brainstem slices were acquired at 4× magnification, with a numerical aperture of 0.20. Images focusing on the region of interest were acquired at 10× magnification, with a numerical aperture of 0.30.

Electrophysiology

For electrophysiological recording, an isolated brainstem was transferred to a low-volume (0.50 ml) flow-through Plexiglas recording chamber. The isolated brainstem was supported ventral side up between coarse nylon mesh allowing the entire surface to be bathed with aCSF from rostral to caudal regions at a rate of 5 ml min^{-1}. Supply of aCSF, equilibrated with an O_2−CO_2 mixture to produce the desired pH, flowed through plastic tubing to the chamber. After dissection, the brainstem was allowed to stabilize for 1 h at 25°C, pH 7.8 and ~ 11 Torr P_{co_2}. CO_2 was analyzed with a Datex 223 CO_2 Monitor (Puritan-Bennett Corp., Pleasanton, CA, USA).

Roots of the facial and hypoglossal nerves were drawn into glass suction electrodes pulled from 1-mm-diameter capillary glass to tip diameters of 30–60 μm. Whole-nerve discharge was amplified (100× by a DAM-50 amplifier, World Precision Instruments, Sarasota, FL, USA; and then 1,000× by model 1,700 differential AC amplifier; A-M Systems, Carlsborg, WA), and filtered (100 Hz high-pass and 1,000 Hz low-pass by the second amplifier). The amplified and filtered output was sent to a data acquisition system (Powerlab, AD Instruments, Colorado Springs, CO), which sampled data at 1 kHz, integrated data (full-wave rectified and averaged over 200 ms), as well as recorded and archived the whole-nerve discharge as neurograms.

The neurograms recorded from the facial and hypoglossal nerves consisted of rhythmic activity in two forms: low amplitude, high frequency bursts representing buccal ventilation and high amplitude, low frequency bursts representing lung ventilation (Gdovin et al. 1996). The present investigation focused on lung respiratory rhythm and episodic pattern generation.

NIH-PA Author Manuscript

NIH-PA Author Manuscript

NIH-PA Author Manuscript

Following stabilization for 60 min, baseline nerve activity was recorded for 30 min, during which the brain-stem was superfused with aCSF at pH 7.8 equilibrated with 1.5% CO_2, balance O_2. The brainstem was treated for 30 min with bath application of an agonist and followed by 30 min with bath application of an antagonist for the receptor of interest. The preparation then underwent a 30-min washout period. For NK1R receptor studies, preparations were superfused with 5.0 μM SP and 750 nM antagonist D (n = 7). For μOR studies, preparations were superfused with 100 nM DAMGO and 1.0 μM naloxone (n = 5). These concentrations were chosen based on previous studies of bullfrog neuroventilation (Chen and Hedrick 2008; Vasilakos et al. 2005). The neuromodulators DAMGO ([D-Ala^2, N-Me-Phe^4, Gly^5-ol]-Enkephalin acetate salt), antagonist D ([D-Arg^1, D-Phe^5, D-Trp^{7,9}, Leu^{11}]-substance P), SP acetate salt hydrate and naloxone hydrochloride dehydrate were all purchased from Sigma Chemical (St Louis, MO, USA).

Data analysis and statistics

Immunofluorescence—Color was added to the individual channels using Image J software (a public domain image processing program developed at the National Institutes of Health), and colocalization images were generated by overlaying the individual channels with ColocalizerPro (Colocalization Research Software, Apple, Cupertino, CA, USA). Colocalization was quantified with two colocalization coefficients, Pearson's correlation coefficient and overlap coefficient according to Manders. Pearson's correlation coefficient is one of the standard measures in pattern recognition and is used for describing the correlation of the intensity distributions between channels. It takes into consideration only similarity between shapes, while ignoring the intensities of signals.

The Pearson's correlation coefficient ranges from −1 to 1. A value of −1 indicates no correlation in fluorescence localization, and a value of 1 indicates a perfect correlation between the two channels. The overlap coefficient according to Manders indicates an overlap of the signal and represents the true degree of colocalization. It ranges from 0 to 1. A value of 0 indicates that none of the image pixels overlap, while a value of 0.7, for example, indicates that 70% of the pixels overlap. Colocalization coefficients were calculated after background correction using ColocalizerPro. Both colocalization coefficients indicate the presence of receptor colocalization, but do not indicate the number of receptors present in the colocalized region. Fluorescence intensity of receptor-antibody staining was calculated by the Image **J** software. Fluorescent images were captured with a 16-bit camera which registered variations in fluorescence as 65,536 levels of gray (grayscale values for each pixel). Fluorescence intensity of receptor-antibody staining was measured in grayscale values corrected for background fluorescence. Grayscale values for each image were generated by Image **J**. One-way analysis of variance (ANOVA) followed by a Student-Newman-Keuls multiple comparison test was used to determine statistical differences in the mean colocalization coefficients and mean fluorescence intensities.

Electrophysiology—Analysis of neurograms focused on changes in lung ventilation due to the focus on the lung RRG in relation to immunohistochemical studies performed. Lung burst frequency was determined by counting the number of lung bursts per minute for every minute of each 30-min treatment and control/baseline period. For each 30-min period the number of lung bursts per episode, the episode frequency and lung burst cycle frequency (BCF) was calculated over the last 3 mins of the period. BCF was calculated as the inverse of the period between the start of one lung burst to the start of the next lung burst. Lung burst parameters including duration, amplitude, and area were quantified over the last 3 min of each period. Analysis of lung neuroventilation was divided into four categories: baseline, agonist, antagonist, and washout. Because BCF and lung burst parameters changed steadily over the 30-min treatment periods, they were quantified once over 3-min at the end of the

NIH-PA Author Manuscript

NIH-PA Author Manuscript

NIH-PA Author Manuscript

treatment periods. Graphs were generated using SigmaPlot (Systat Software Inc., San Jose, CA, USA) and statistical analyses were conducted with SigmaStat (Systat Software Inc., San Jose, CA). One-way repeated measures analysis of variance (RM-ANOVA) followed by a Student-Newman-Keuls multiple comparison test was used to determine statistical differences in the burst and episode parameters of each 30-min treatment. All data are reported as mean ± SEM.

Results

NK1R and μOR colocalization

All cross-section slices from eight juvenile frogs and six early-, middle-, and late-stage tadpoles were visually inspected via fluorescence microscopy with the aim of identifying distinct areas of colocalization of NK1R and μOR antibody staining. Colocalization was evident in the brainstem of all bullfrog stages; however, only juvenile bullfrog brainstems exhibited a consistent and distinct area of colocalization. All eight juvenile brainstems exhibited NK1R and μOR colocalization near the ventral surface of the brainstem caudal to the auditory nerve (Fig. 1a, b, c). On average, ten of the slices from each brainstem observed contained the region of colocalization, making the region approximately 160 μm in length along rostral-caudal axis. Of the eight juvenile brainstems imaged, three exhibited additional areas of colocalization closer to the dorsal surface near the facial motor and auditory nuclei.

The approximate location of the colocalization in juvenile brainstems, the region of interest, was measured consistently on the right half of the slice. The region of interest was a rectangle whose borders were 390.7 ± 66.7 μm from the dorsal surface, 172.5 ± 26.6 μm from the ventral surface, 666.5 ± 26.6 μm from the midline and 503.5 ± 68.2 μm from the right edge of the slices of the medulla. This is a region just caudal to the auditory nerve, if one is using external landmarks, or near the nucleus reticularis parvocellularis (see Adli et al. 1999) if one is a using brainstem nuclei as landmarks. The height and width of the region of interest were calculated as 261.8 ± 8.9 μm and 235.9 ± 21.6 μm, respectively.

Colocalization was quantified based on two colocalization coefficients. Region of interest colocalization coefficients were computed for each of the eight juvenile bullfrog brainstems. The Pearson's correlation coefficient (Rr) was 0.79 ± 0.03 and the overlap coefficient according to Manders (*R*) was 0.90 ± 0.02.

Ontogeny of NK1R and μOR colocalization

Pearson's correlation coefficient and overlap coefficient according to Manders was measured for early-, middle-, and late-stage tadpoles ($n = 6$ for each group) in the region of interest identified in juvenile bullfrog brainstems. The mean Pearson's coefficients for early-, middle-, and late-stage tadpoles were 0.80 ± 0.03, 0.81 ± 0.03, and 0.78 ± 0.03, respectively. The overlap coefficient according to Manders for early-, middle-, and late-stage tadpoles were 0.95 ± 0.02, 0.98 ± 0.01 and 0.92 ± 0.02, respectively. Thus, neither colocalization coefficient changed significantly with development.

Despite having NK1R and μOR colocalization in the region of interest that was similar to that of juvenile bullfrogs, consistent and distinct areas of colocalization could not be identified during our visual inspection of the cross-section slices of early-, middle-, and late-stage tadpoles. In addition to the region of interest, there was consistent colocalization of NK1R and μOR antibody staining in the midline raphe of the tadpole medulla. The colocalization coefficients measured in the raphe areas were not significantly different from those of the region of interests ($P > 0.05$). There were also consistent areas where the colocalization coefficients were lower than the region of interest. For example, as an equal-

NIH-PA Author Manuscript

NIH-PA Author Manuscript

NIH-PA Author Manuscript

sized area immediately lateral to the region of interest had significantly lower ($P < 0.05$) Pearson's coefficients and overlap coefficients according to Manders. However, the distinctness of the areas of both high and low colocalization was weakened by sporadic areas of high colocalization, which occurred in tadpole brainstems.

NK1R and μOR intensity

For six early-, middle-, and late-stage tadpoles and eight juvenile frogs, the mean fluorescence intensity for NK1R-antibody staining in the region of interest was 646.9 ± 74.1, 505.2 ± 34.7, 1,106.2 ± 154.1 and 787.7 ± 38.9, respectively (Fig. 1d). The intensity of fluorescence based on NK1R antibody binding was significantly different in the brainstems of middle-stage tadpoles compared to that of late-stage tadpoles ($P < 0.05$). All other groupings of tadpole and bullfrog stages comprised statistically homogenous subsets.

For six early-, middle-, and late-stage tadpoles and eight juvenile frogs, the mean fluorescence intensities for μOR-antibody staining in the region of interest were 292.6 ± 39.1, 300.6 ± 26.6, 391.4 ± 60.7, and 612.4 ± 33.2, respectively (Fig. 1e). There was a significant difference in the intensity of μOR-antibody staining between juvenile bullfrogs and all tadpole stages.

Role of NK1R in bullfrog neuroventilation

Juvenile bullfrog lung burst parameters—Isolated brainstems of juvenile bullfrogs underwent 30 min of the following: baseline, 5.0 μM SP, 750 nM antagonist D, and washout. Mean lung frequency at baseline was 5.8 ± 0.2 bursts min^{-1}, while frequency during SP exposure increased significantly to 10.3 ± 0.5 bursts min^{-1} ($P < 0.00$, Fig. 2a, e). During subsequent bath application of antagonist D the lung frequency significantly decreased to 5.8 ± 0.2 bursts min^{-1} ($P < 0.001$), and returned to baseline levels during washout (data not shown).

Lung burst area increased significantly from a baseline value of 0.02 ± 0.001 to 0.02 ± 0.001 V s during SP ($P < 0.001$, Fig. 2b), and it increased, again significantly, during antagonist D treatment (0.03 ± 0.003 V s, $P < 0.001$). SP decreased lung burst duration from a baseline of 1.1 ± 0.1−0.9 ± 0.02 s ($P = 0.005$, Fig. 2c). During antagonist D exposure lung burst duration significantly increased to 1.2 ± 0.9 s ($P < 0.001$), which was equivalent to duration during baseline. Lung burst amplitude during baseline was 0.05 ± 0.003 V and significantly increased to 0.07 ± 0.002 V ($P < 0.001$, Fig. 2d) during SP application and remained significantly higher than baseline during antagonist D treatment (0.07 ± 0.004 V).

Early-stage tadpole lung burst parameters—Isolated brainstems of early-stage tadpoles ($n = 6$) underwent 30 min of the following: baseline, 5.0 μM SP, 750 nM antagonist D and washout. SP significantly increased lung burst frequency (lung burst min^{-1}) from a baseline of 1.4 ± 0.2−3.8 ± 0.3 bursts min^{-1} ($P < 0.001$, Fig. 3a, b). During subsequent exposure to antagonist D, lung burst frequency significantly decreased to a baseline level of 2.0 ± 0.2 bursts min^{-1} ($P < 0.001$).

Juvenile bullfrog episode parameters—BCF was not affected by SP treatment; the baseline 56.7 ± 1.5 and the BCF 58.0 ± 1.5 bursts min^{-1} during SP application (Fig. 4a) was not significantly different. Neither was affected by antagonist D treatment; it was 53.3 ± 2.4 bursts min^{-1} during treatment, which was equivalent to baseline.

Episode frequency (episodes min^{-1}) calculated for each treatment period showed a significant increase with SP exposure followed by a significant decrease during antagonist D application (Fig. 4b). Episode frequency increased from 3.7 ± 0.1 episodes min^{-1} during

NIH-PA Author Manuscript

NIH-PA Author Manuscript

NIH-PA Author Manuscript

baseline to 7.1 ± 0.3 episodes min^{-1} during SP exposure ($P < 0.05$). Episode frequency decreased during antagonist D treatment to 4.5 ± 0.2 episodes min^{-1} ($P < 0.05$), which was equivalent to baseline.

The number of lung bursts per episode during baseline was 1.6 ± 0.03 bursts $episode^{-1}$ (Fig. 4c). During bath application of SP, the number of lung bursts per episode underwent a very small, albeit statistically significant, decrease to 1.5 ± 0.02 bursts $episode^{-1}$ ($P < 0.05$). During subsequent exposure to antagonist D, the number of lung bursts per episode decreased, again significantly, to 1.3 ± 0.03 bursts $episode^{-1}$ ($P < 0.05$). During baseline and treatment with SP and antagonist D episodes of a single burst made up the highest percentage of episodes. The percentage of single-burst episodes increased from 34% to 47% to 79% during baseline, SP and antagonist D treatments, respectively.

Role of μOR in bullfrog neuroventilation

Juvenile bullfrog lung burst parameters—Juvenile bullfrogs ($n = 5$) underwent 30 min of the following: baseline, 100 nM DAMGO, 1.0 μM naloxone and washout. Lung frequency during baseline was 7.5 ± 0.5 bursts min^{-1} and significantly decreased to 4.2 ± 0.4 bursts min^{-1} during DAMGO exposure ($P < 0.001$, Fig. 5a, e). During naloxone exposure lung frequency significantly increased to 5.3 ± 0.4 bursts min^{-1} ($P = 0.001$), but did not restore frequency to baseline levels ($P < 0.001$). Thus, naloxone appears to reverse the effect of DAMGO in that there was a significant increase in lung burst frequency during its application which followed DAMGO application. However, since lung burst frequency did not return baseline levels, the duration of its application was likely not enough time for complete washout of DAMGO. This is further evidenced by the continued decrease in lung burst amplitude, duration, and area. Lung burst parameters returned to baseline levels during washout. Lung burst frequency returned to baseline levels during washout (data not shown).

Lung burst area reached its greatest values during DAMGO exposure with a mean area of 0.02 ± 0.001 V s, a significant increase from baseline areas of 0.01 ± 0.001 V s ($P < 0.05$, Fig. 5b). The lowest value of lung burst area was during naloxone, which decreased to 0.01 ± 0.001 V s. Duration decreased significantly to 0.6 ± 0.01 s during naloxone exposure ($P < 0.001$, Fig. 5c). Lung burst amplitude also increased significantly from 0.04 ± 0.002 to 0.06 ± 0.003 V during DAMGO ($P < 0.05$) and decreased to 0.05 ± 0.002 V ($P < 0.05$, Fig. 5d) during naloxone.

Early-stage tadpole lung burst parameters—Isolated brainstems of early-stage tadpoles ($n = 6$) underwent 30-min of the following: baseline, 100 nM DAMGO, 1.0 μM naloxone and washout. Lung burst frequency significantly decreased from a baseline of 1.5 ± 0.1 to 1.1 ± 0.1 bursts min^{-1} during DAMGO bath application ($P = 0.011$, Fig. 6a, b). Frequency increased significantly during subsequent naloxone exposure to 2.9 ± 0.3 bursts min^{-1} ($P < 0.001$), a level significantly greater than baseline ($P < 0.001$). Lung burst frequency significantly decreased during washout ($P < 0.05$), but did not return to baseline levels ($P > 0.05$).

Juvenile bullfrog episode parameters—A significant decrease in lung burst cycle frequency (BCF) was observed during DAMGO exposure, a decrease to 48.4 ± 1.3 bursts min^{-1} from a baseline of 61.4 ± 1.7 bursts min^{-1} ($P < 0.05$, Fig. 7a). Subsequently, during application of naloxone, BCF increased significantly to 70.8 ± 1.2 bursts min^{-1} ($P < 0.001$), a value significantly greater than baseline ($P < 0.05$).

NIH-PA Author Manuscript

NIH-PA Author Manuscript

NIH-PA Author Manuscript

DAMGO significantly decreased episode frequency from a baseline of 2.6 ± 0.1 to 1.9 ± 0.1 episodes min^{-1} ($P < 0.05$, Fig. 7b). Naloxone slightly raised episode frequency to 2.0 ± 0.1 episodes min^{-1}, though this value differed significantly from baseline ($P < 0.05$).

The mean number of lung bursts per episode during baseline was 2.7 ± 0.1 (Fig. 7c). This value decreased significantly during DAMGO exposure to 2.2 ± 0.1 ($P < 0.001$). Lung bursts per episode increased to 2.6 ± 0.1 during naloxone treatment, though this value was significantly lower than baseline ($P < 0.001$). During all treatments, episodes containing two bursts made up the highest percentage of episodes. The percentage of episodes with two bursts decreased from 47% during baseline to 43% with DAMGO and 31% during naloxone.

Discussion

This study demonstrated that NK1R and μOR neuromodulators influence the lung ventilatory rhythm and episodic pattern in bullfrogs. Ligand binding at NK1R and μOR influences the number of lung bursts present in each episode, lung burst parameters, the lung burst cycle frequency, as well as the frequency of episodes. The role of NK1R and μOR in bullfrog neuroventilation is consistent throughout development with SP (the NK1R agonist) eliciting an increase in lung burst frequency whereas DAMGO (the μOR agonist) depresses lung burst frequency. Based on immunofluorescent double-labeling, we have identified a population of NK1R and μOR co-expressing neurons located in or near a region identified as the location of the respiratory rhythm generator (RRG, Wilson et al. 2002). We hypothesize that these neurons correspond to the RRG neurons, and having an anatomical marker we can address this as a question. NK1R and μOR colocalization is a marker of the mammalian pre-Bötzinger complex (PBC, Gray et al. 1999). If the NK1R and μOR co-expressing neurons that we have identified are lung RRG neurons, then the bullfrog lung RRG is potentially homologous or homoplastic with the mammalian PBC. The putative lung RRG is a bilaterally paired structure located caudal to the auditory nerves in the ventral half of the medulla half way between the midline and the edges of the brainstem. As such, our findings support the location of a lung RRG proposed by Wilson et al. (2002) and the homology proposed by Vasilakos et al. (2005) and Wilson et al. (2006), and thus the focus of this research was on drug-induced changes in lung ventilation rather than buccal ventilation.

Immunofluorescence of the putative lung RRG

High densities of NK1R within the PBC colocalize with μOR (Gray et al. 1999) and are used to locate the PBC on mammalian brainstem slices. Similar respiratory responses of bullfrogs and mammals to SP and DAMGO suggest that colocalization of these receptors will mark the putative lung RRG of bullfrogs. Lack of buccal response to DAMGO (Vasilakos et al. 2005) suggests that colocalization of these receptors will not mark the putative buccal RRG in bullfrog brainstem slices.

One bilaterally paired area of colocalization, which was both visually distinct and consistent among animals, was found in the juvenile bullfrog brainstem. These colocalized receptors were located caudal to the auditory nerve root, near the facial nucleus. This area was visually distinct in slices from juveniles because it was typically the only area of colocalization and staining for the μOR was its most intense in this area. Wilson et al. (2002) used injections of AMPA and GABA into this region to induce increases and decreases, respectively, in lung burst frequency, and thereby linked this area with bullfrog lung respiratory rhythm generation. Demonstrating that lung burst frequency is influenced by injection of DAMGO and SP into the proposed site of the lung RRG would give further evidence that the colocalized area marks the lung RRG in bullfrogs, as bath application of drugs is a limitation of this study.

NIH-PA Author Manuscript

NIH-PA Author Manuscript

NIH-PA Author Manuscript

The bilaterally paired area of colocalization that was visually distinct in juvenile bullfrogs was also present in brainstem slices from early-, middle- and late-stage tadpoles, which is consistent with the common response to SP and DAMGO exhibited by tadpoles and juvenile bullfrogs. The lack of visual distinctness of this area in tadpole brainstems was due to the fact that NK1R and μOR colocalization was common in other areas, but not consistent among all animals or developmental stages. This may indicate additional roles of NK1R and μOR in neural development or physiological behaviors moderated by the brainstem, but our data do not support speculation on a specific function. Changes in NK1R intensity in the putative lung RRG did not correlate with development, perhaps suggesting a consistent role of NK1R in lung ventilation. In contrast, μOR intensity in the putative lung RRG increased at metamorphosis. In the mammalian PBC the expression of μOR increases dramatically between P6 and P15, and the total μOR increases with age (Wong-Riley and Liu 2005). Thus, the role of μOR in activity of the putative lung RRG and the PBC may change with development, indicated by an increase in receptor intensity but no changed response to DAMGO, and warrants further investigation.

Lung neuroventilatory response to SP

The response to SP is well documented in mammals. SP modulates activity of the rhythm generator in newborn rats (Ptak et al. 1999), and changes in the level of SP in the nucleus tractus solitarius have suggested a role for SP in regulating the onset of breathing (Srinivasan et al. 1991). In vitro brainstem preparations of the newborn rat exhibit increased respiratory frequency with SP treatment (Yamamoto et al. 1992). Blockade of SP receptors with spantide results in significant irregular breathing activity and decreased frequency in control mice (Telgkamp et al. 2002), suggesting a role of endogenous SP in the regularity and frequency of normal respiration.

SP has similar influences through bullfrog and mammalian ontogeny. SP has been shown previously to increase lung burst frequency in isolated brainstems from pre- and post-metamorphic bullfrog tadpoles and adults (Chen and Hedrick 2008) and that finding is confirmed here for early-, middle-, and late-stage tadpoles and juvenile bullfrogs. The significant increase in lung burst frequency with bath application of SP to juvenile bullfrog and tadpole brainstems suggests that NK1R receptors play a role in regulating respiratory rhythm throughout development. Injection of SP conjugated with saporin, which specifically destroys NK1R-expressing neurons (Mantyh et al. 1995, 1997), into the PBC of adult rats produces abnormal breathing periods (Wang et al. 2002). Given the established similarities between mammalian and amphibian neuronal networks, along with results from this study, it is possible that lesions of NK1R in our putative lung RRG, which we suggest is the same as the Wilson et al. (2002) area, will also produce abnormal breathing periods.

Episodes can consist of one or a number of lung bursts, and the duration of the episode changes with changes in respiratory drive (for review see Kinkead 1997). Lung burst frequency increases with SP and returns to baseline during antagonist D treatment. Interestingly, both SP and antagonist D decrease the number of lung bursts per episode, while episode frequency increases with SP and returns to baseline during antagonist D application. The decreases in the number of bursts per episode, however, were one and two tenths of a breath for SP and antagonist D respectively, which seems unlikely to have any relevant physiological impact. This suggests that SP does not enhance respiratory drive in a way that increases the number of lung bursts per episode; rather it increases respiratory drive such that there are more frequent episodes. SP application leads to more single breaths and fewer episodes of multiple breaths. The implication is that NK1R are involved in respiratory-related output by increasing the frequency of episodes and the production of episodes with higher numbers of lung bursts. These data support the hypothesis discussed by Kinkead et al. (1994) that episodic pattern generation is an intrinsic property of the central

NIH-PA Author Manuscript

NIH-PA Author Manuscript

NIH-PA Author Manuscript

respiratory control network, but offer no insight as to the specific location of an episodic pattern generator since NK1R are distributed throughout the brainstem.

Episodic pattern generation in bullfrog neuroventilation can be separated from rhythm generation. Eliminating the clustering of lung breaths into episodes without changing lung burst frequency or, presumably, respiratory drive, is possible with application of the $GABA_B$ agonist baclofen (Straus et al. 2000a, b). A similar bath application of a neuronal nitric oxide synthase (nNOS) inhibitor found that nNOS inhibition reduces the number of breaths per episode, and produces single breaths rather than clusters, without an overall change in frequency (Harris et al. 2002). Our bath application of SP, however, was inconclusive in terms of separating rhythm and episodic pattern generation. SP decreased the number of lung bursts per episode, but the overall lung burst frequency and episode frequency increased with SP. This suggests that SP may act directly on the mechanisms responsible for episodic pattern generation. Given that SP increases lung burst frequency in early-stage tadpole brainstems, the role of NK1R and developmental changes in their abundance and distribution warrants further investigation.

Changes in lung burst parameters including frequency, duration, amplitude, and area indicate changes in respiratory drive caused by influences on the RRG. SP significantly decreases lung burst duration. This effect is not surprising when evaluated with the significant increase in lung burst frequency. The decrease in lung burst duration allows for subsequent breaths to follow at a quicker rate, thus increasing absolute frequency. In anurans, lung burst area has been associated with respiratory tidal volume (McAneney and Reid 2007). The increase in area during SP treatment despite the decrease in lung burst duration is attributed to the increase in lung burst amplitude. Despite the shorter duration, the lung bursts are stronger than baseline, allowing for a greater area. The significant increase in area during antagonist D is attributed to the larger duration, which returned to baseline levels, together with the larger amplitude, which remained constant after SP application.

Lung neuroventilatory response to μ-opiates

Bullfrog neuroventilation typically occurs as a combination of buccal and lung bursts. Despite being timed to one another, there is evidence to suggest that buccal and lung bursts are controlled in different areas of the brainstem (Wilson et al. 2002) and are influenced differently by a variety of chemicals. Treatment with μ-opiates (morphine or DAMGO) is one means to uncouple the buccal and lung oscillators of bullfrogs (Vasilakos et al. 2005), just as it uncouples respiratory oscillators in the rat brainstem (Mellen et al. 2003). Bath application of DAMGO to bullfrog brainstems results in a significant decrease in lung neuroventilation, suggesting that μOR have a role in modulating lung respiratory rhythm. These results are consistent with those of Vasilakos et al. (2005) who showed that the overall frequency of lung bursts decreased with application of DAMGO. These authors found that buccal burst frequency remained constant in both stages of animals. In intact bullfrogs, morphine injection significantly decreased lung ventilation, but the total number of ventilatory events (buccal plus lung) remained constant (Vasilakos et al. 2005); therefore, buccal ventilation replaced lung ventilation under the influence of μ-opiates.

Data from our study confirms the depression in lung ventilation with DAMGO treatment and shows recovery from the depressive effects during subsequent treatment with naloxone.

DAMGO decreases the absolute lung burst frequency while also decreasing the number of lung bursts per episode and the episode frequency. While there is a change in episodic pattern, owing to fewer bursts per episode, there is also an overall decrease in respiratory drive indicated by the decrease in lung burst and episode frequencies. Duration and

NIH-PA Author Manuscript

NIH-PA Author Manuscript

NIH-PA Author Manuscript

amplitude increase during DAMGO treatment, leading to an increase in area. One could speculate that these parameters increase to compensate for the significant decrease in lung burst frequency; a metabolically adequate level of gas exchange may be maintained during respiratory depression by increasing the duration and amplitude of each breath to increase area/tidal volume. Regardless of the functional basis for the increase in area, the results suggest that DAMGO does not directly influence the mechanisms responsible for episodic pattern generation, but influences the overall drive to produce a respiratory rhythm.

Overall, this study confirms the similarity of responses to DAMGO and SP exhibited by juvenile and larval bullfrog in vitro brainstem preparations and uses double-label immunofluorescent binding at the receptors for these neuroactive molecules to mark the location of these receptors in the brainstem. This location may be the site of the bullfrog lung RRG. Furthermore, we have shown that μOR influences episodic pattern generation by affecting the overall respiratory rhythm generation.

Acknowledgments

This work was funded by NIH-NINDS 2U54NS041069-06AI. Protocols used in this study follow the institutional animal care and use committee (IACUC) guidelines and adhere to local and national ethical standards.

References

Adli DSH, Steusse SL, Cruce WLR. Immunohistochemistry and spinal projections of the reticular formation in the northern leopard frog, *Rana pipiens*. J Comp Neurol. 1999; 404:387–407. [PubMed: 9952355]

Bayliss D, Viana F, Berger A. Mechanisms underlying excitatory effects of thyrotropin-releasing hormone on rat hypoglossal motoneurons in vitro. J Neurophysiol. 1992; 68:1733–1745. [PubMed: 1479442]

Belzile O, Gulemetova R, Kinkead R. Role of 5HT2A/C receptors in serotonergic modulation of respiratory motor output during tadpole development. Respir Physiol Neurobiol. 2002; 133:277–282. [PubMed: 12425975]

Chen A, Hedrick M. Role of glutamate and substance P in the amphibian respiratory network during development. Respir Physiol Neurobiol. 2008 doi:10-1016/j.resp.2008.03.010.

Chen Z, Hedner T, Hedner J. Local application of somatostatin in the rat ventrolateral brain medulla induces apnea. J Appl Physiol. 1990; 69:2233–2238. [PubMed: 1981770]

Dong X, Feldman J. Modulation of inspiratory drive to phrenic motoneurons by presynaptic adenosine A1 receptors. J Neurosci. 1995; 15:3458–3467. [PubMed: 7538560]

Folbergrova J, Norberg K, Quistorff B, Siesjo B. Carbohydrate and amino acid metabolism in rat cerebral cortex in moderate and extreme hypercapnia. J Neurochem. 1975; 25:457–462. [PubMed: 1151381]

Galante R, Kubin L, Fishman A, Pack A. Role of chloridemediated inhibition in respiratory rhythmogenesis in an in vitro brainstem of tadpole, *Rana catesbeiana* . J Physiol. 1996; 492:545–558. [PubMed: 9019549]

Gdovin M, Torgerson C, Remmers J. Characterization of gill and lung ventilatory activity in cranial nerves in the spontaneously breathing tadpole, *Rana catesbeiana* . FASEB J. 1996; 10:A642.

Gray P, Rekling J, Bocchiaro C, Feldman J. Modulation of respiratory frequency by peptidergic input to rhythmogenic neurons in the preBötzinger complex. Science. 1999; 286:1566–1568. [PubMed: 10567264]

Gray P, Janczewski W, Mellen N, McCrimmon D, Feldman J. Normal breathing requires preBötzinger complex neurokinin-1 receptor-expressing neurons. Nat Neurosci. 2001; 4:927–930. [PubMed: 11528424]

Guyenet P, Mulkey D, Stornetta R, Bayliss D. Regulation of ventral surface chemoreceptors by the central respiratory pattern generator. J Neurosci. 2005; 25:8938–8947. [PubMed: 16192384]

NIH-PA Author Manuscript

NIH-PA Author Manuscript

NIH-PA Author Manuscript

Harris M, Wilson R, Vasilakos K, Taylor B, Remmers J. Central respiratory activity of the tadpole in vitro brain stem is modulated diversely by nitric oxide. Am J Regulatory Int Comp Physiol. 2002; 283:R417–R428.

Jackson, D. Respiratory control in air breathing ectotherms. In: Davies, D.; Barnes, C., editors. Regulation of ventilation and gas exchange. Dublin: Academic Press; 1978. p. 93-130.

Kazemi H, Hoop B. Glutamic acid and gamma-aminobutyric acid neurotransmitters in central control of breathing. J Appl Physiol. 1991; 70:1–7. [PubMed: 1672687]

Kinkead R. Episodic breathing in frogs: converging hypotheses on neural control of respiration in air breathing vertebrates. Amer Zool. 1997; 37:31–40.

Kinkead R, Milsom W. Chemoreceptors and control of episodic breathing in the bullfrog (*Rana catesbeiana*). Respir Physiol. 1994; 95:81–98. [PubMed: 8153454]

Kinkead R, Milsom W. CO_2-sensitive olfactory and pulmonary receptor modulation of episodic breathing in bullfrogs. Am J Physiol. 1996; 270:R134–R144. [PubMed: 8769795]

Kinkead R, Milsom W. Role of pulmonary stretch receptor feedback in the control of episodic breathing in the bullfrog. Am J Physiol. 1997; 272:R497–R508. [PubMed: 9124470]

Kinkead R, Filmyer W, Mitchell G, Milsom W. Vagal input enhances responsiveness of respiratory discharge to central changes in pH/CO2 in bullfrogs. J Appl Physiol. 1994; 77:2048–2051. [PubMed: 7836236]

Liu Y, Wong-Riley M, Liu J, Wei X, Jia Y, Liu H, Fujiyama F, Ju G. Substance P and enkephalinergic synapses onto neurok-inin-1 receptor-immunoreactive neurons in the pre-Bötzinger complex of rats. Eur J Neurosci. 2004; 19:65–75. [PubMed: 14750964]

Llona I, Ampuero E, Eugenin J. Somatostatin inhibition of fictive respiration is modulated by pH. Brain Res. 2004; 1026:136–142. [PubMed: 15476705]

Maggi C, Patacchini R, Rovero P, Giachetti A. Tachykinin receptors and tachykinin receptor antagonists. J Auton Pharmacol. 1993; 13:23–93. [PubMed: 8382703]

Mantyh P, DeMaster E, Malhotra A, Ghilardi J, Rogers S, et al. Receptor endocytosis and dendrite reshaping in spinal neurons after somatosensory stimulation. Science. 1995; 268:1629–1632. [PubMed: 7539937]

Mantyh P, Rogers D, Monroe P, Allen B, Rea Ghilardi. Inhibition of hyperalgesia by ablation of lamina I spinal neurons expressing the substance P receptor. Science. 1997; 278:275–279. [PubMed: 9323204]

McAneney J, Reid S. Chronic hypoxia attenuates central respiratory-related pH/CO2 chemosensitivity in the cane toad. Resp Physiol Neurobiol. 2007; 156:266–275.

Mellen N, Janczewski W, Bocchiaro C, Feldman J. Opioid-induced quantal slowing reveals dual networks for respiratory rhythm generation. Neuron. 2003; 37:821–826. [PubMed: 12628172]

Metz B. Hypercapnia and acetylcholine release from the cortex and medulla. J Physiol Lond. 1966; 186:321–322. [PubMed: 5972111]

Nattie E, Li A. Substance P-saporin lesion of neurons with NK1 receptors in one chemoreceptor site in rats decreases ventilation and chemosensitivity. J Physiol. 2002; 544:603–616. [PubMed: 12381830]

Nattie E, Prabhakar N. Peripheral and central chemosensitivity: multiple mechanisms, multiple sites? A workshop summary. Adv Exp Med Biol. 2001; 499:73–80. [PubMed: 11729937]

Onimaru H, Arata A, Homma I. Intrinsic burst generation in pre-inspiratory neurons in the medulla of brainstem-spinal cord preparations isolated from newborn rats. Exp Brain Res. 1995; 106:57–68. [PubMed: 8542977]

Onimaru H, Arata A, Homma I. Neuronal mechanisms of respiratory rhythm generation; an approach using in vitro preparation. Jpn J Physiol. 1997; 47:385–403. [PubMed: 9504127]

Ptak K, Di Pasquale E, Monteau R. Substance P and central respiratory activity: a comparative in vitro study on fetal and newborn rat. Brain Res Dev Brain Res. 1999; 114:217–227.

Rekling J. Excitatory effects of thyrotropin-releasing hormone (TRH) in hypoglossal motoneurons. Brain Res. 1990; 510:175–179. [PubMed: 2108785]

Rekling J, Feldman J. PreBötzinger Complex and pacemaker neurons: hypothesized site and kernel for respiratory rhythm generation. Annu Rev Physiol. 1998; 60:385–405. [PubMed: 9558470]

NIH-PA Author Manuscript

NIH-PA Author Manuscript

NIH-PA Author Manuscript

Smatresk N, Smits A. Effects of central and peripheral chemoreceptor stimulation on ventilation in the marine toad, Bufo marinus. Respir Physiol. 1991; 83:223–238. [PubMed: 1906195]

Smith J, Ellenberger H, Ballanyi K, Richter D, Feldman J. PreBötzinger complex: a brainstem region that may generate respiratory rhythm in mammals. Science. 1991; 254:726–729. [PubMed: 1683005]

Srinivasan M, Goiny M, Pantaleo T, et al. Enhanced in vivo release of substance P in the nucleus tractus solitarius during hypoxia in the rabbit: role of peripheral input. Brain Res. 1991; 546:211–216. [PubMed: 1712658]

Straus C, Wilson R, Remmers J. Developmental disinhibition: turning off inhibition turns on breathing in vertebrates. J Neurobiol. 2000a; 45:75–83. [PubMed: 11018769]

Straus C, Wilson R, Tezenas du Montcel S, Remmers J. Baclofen eliminated cluster lung breathing of the tadpole brainstem, in vitro. Neurosci Lett. 2000b; 292:13–16. [PubMed: 10996438]

Stuesse S, Adli D, Cruce W. Immunochemical distribution of enkephalin, substance P and somatostatin in the brainstem of the leopard frog, *Rana pipiens* . Microsc Res Tech. 2001; 54:229–245. [PubMed: 11514979]

Takeda S, Eriksson L, Yamamoto Y, Joensen H, Onimaru H, Lindahl S. Opioid action on respiratory neuron activity of the isolated respiratory network in newborn rats. Anesthesiology. 2001; 95:740–749. [PubMed: 11575549]

Taylor A, Köllros J. Stages in the normal development of *Rana pipiens* larvae. Anat Rec. 1946; 94:7–24. [PubMed: 21013391]

Taylor B, Harris M, Leiter J, Gdovin M. Ontogeny of central CO_2 chemoreception: chemosensitivity in the ventral medulla of developing bullfrogs. Am J Physiol Regul Integr Comp Physiol. 2003; 285:R1461–R1472. [PubMed: 14615406]

Telgkamp P, Cao Y, Basbaum A, Ramirez J. Long-term deprivation of substance P in PPT-A mutant mice alters the anoxic response of the isolated respiratory network. J Neurophysiol. 2002; 88:206–213. [PubMed: 12091546]

Torgerson C, Gdovin M, Remmers J. Ontogeny of central chemoreception during fictive gill and lung ventilation in an in vitro brainstem preparation of *Rana catesbeiana* . J Exp Biol. 1997; 200:2063–2072. [PubMed: 9319973]

Vasilakos K, Wilson R, Kimura N, Remmers J. Ancient gill and lung oscillators may generate the respiratory rhythm of frogs and rats. J Neurobiol. 2005; 62:369–385. [PubMed: 15551345]

Wang H, Germanson T, Guyenet P. Depressor and tachypneic responses to chemical stimulation of the ventral respiratory group are reduced by ablation of neurokinin-1 receptor-expressing neurons. J Neurosci. 2002; 22:3755–3764. [PubMed: 11978851]

West N, Topor Z, van V, liet B. Hypoxemic threshold for lung ventilation in the toad. Respir Physiol. 1987; 70:377–390. [PubMed: 3120266]

Weyne J, Leuven F, Kazemi H, Leusen I. Selected brain amino acids and ammonium during chronic hypercapnia in conscious rats. J Appl Physiol. 1978; 44:333–339. [PubMed: 632172]

Wilson R, Vasilakos K, Harris M, Straus C, Remmers J. Evidence that ventilatory rhythmogenesis in the frog involves two distinct neuronal oscillators. J Physiol. 2002; 540:557–570. [PubMed: 11956343]

Wilson R, Vasilakos K, Remmers J. Phylogeny of vertebrate respiratory rhythm generators: the oscillator homology hypothesis. Resp Physiol and Neurobiol. 2006; 154:47–60.

Wong-Riley M, Liu Q. Neurochemical development of brain stem nuclei involved in the control of respiration. Resp Physiol and Neurobiol. 2005; 149:83–98.

Yamamoto Y, Onimaru H, Homma I. Effect of substance P on respiratory rhythm and pre-inspiratory neurons in the ventrolateral structure of rostral medulla oblongata: an in vivo study. Brain Res. 1992; 599:272–278. [PubMed: 1283971]

NIH-PA Author Manuscript
NIH-PA Author Manuscript
NIH-PA Author Manuscript

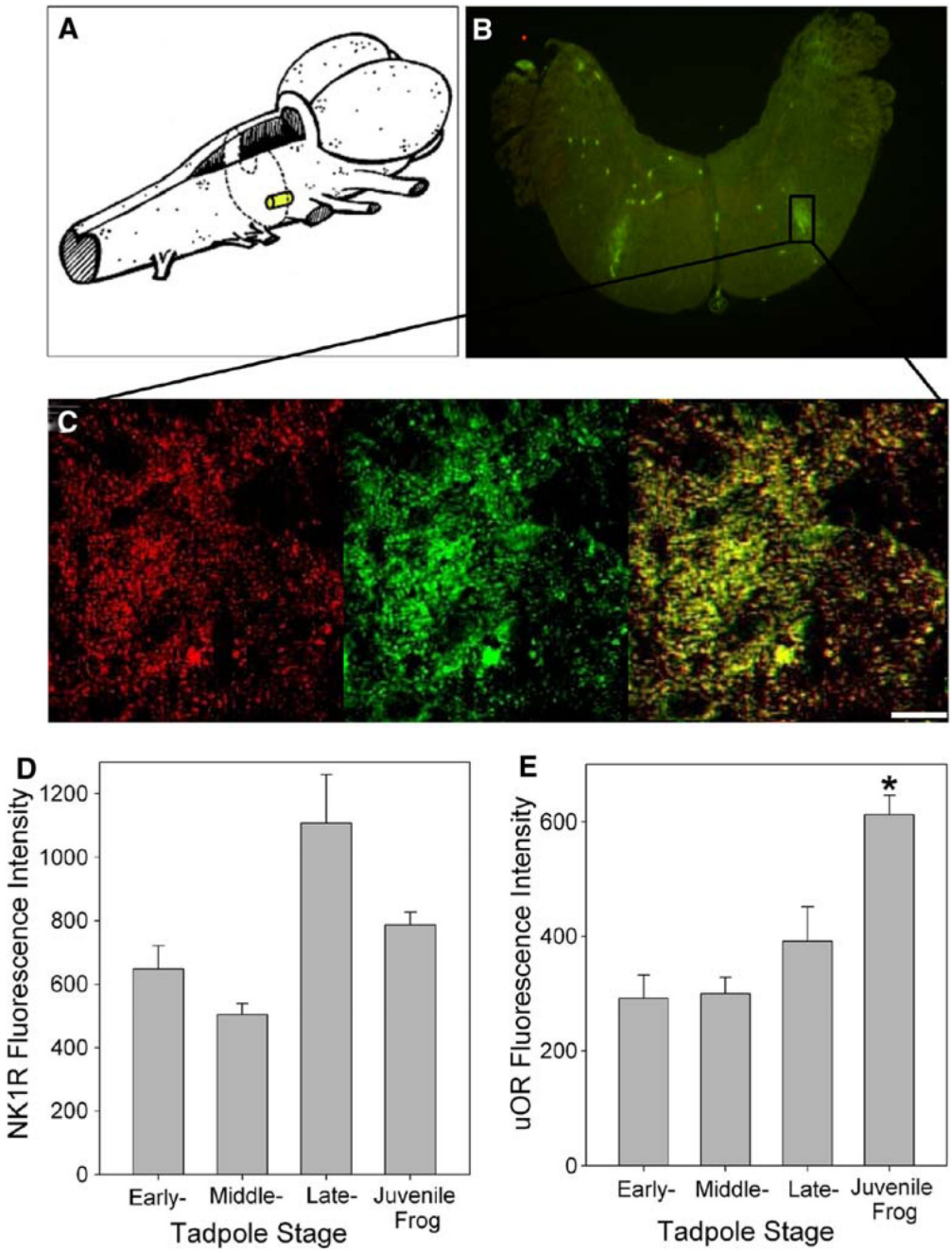

Fig. 1.

NK1R and μOR colocalization in the juvenile bullfrog brainstem. **a** Drawing illustrates the approximate location and size of NK1R and μOR colocalization in the juvenile bullfrog brainstem. **b** NK1R and μOR colocalize on the ventral surface of the brainstem near the facial nucleus in juvenile bullfrog brainstems ($n = 8$). **c** Magnified view of NK1R (*red*) and μOR (*green*) colocalization (*yellow*) in the region of interest. The bar indicates 10 μm. **d** NK1R fluorescence intensity has no developmental trend ($n = 6–8$). **e** μOR fluorescence intensity increased significantly from late-stage tadpole to juvenile bullfrog ($n = 6–8$). Data are mean ± SEM. *Asterisk* indicates a significant difference from all other groups ($P < 0.05$)

NIH-PA Author Manuscript

NIH-PA Author Manuscript

NIH-PA Author Manuscript

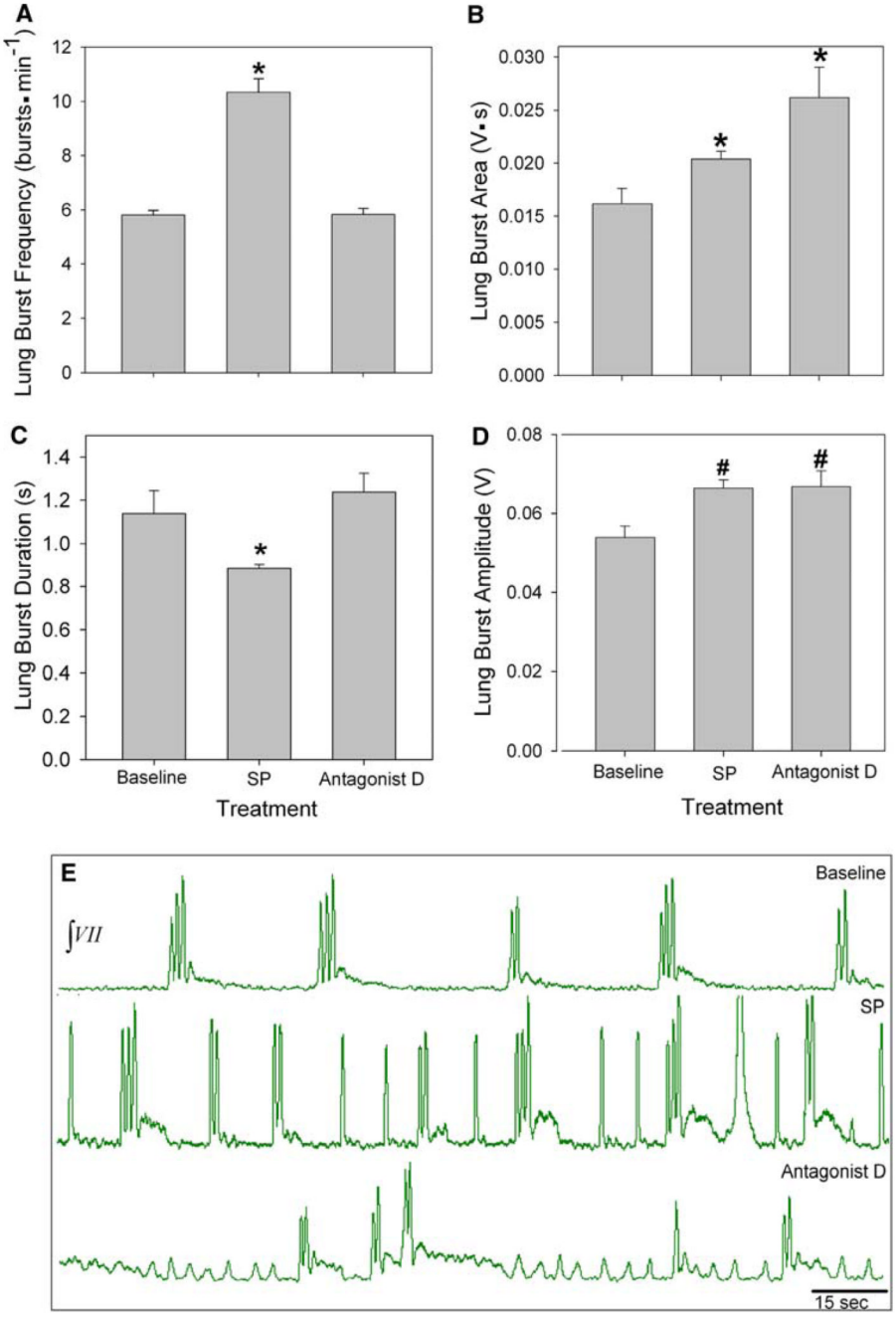

Fig. 2.

Role of NK1R in juvenile bullfrog respiratory rhythm generation. **a** SP significantly increased lung burst frequency and **b** lung bur area. **c** Lung burst duration significantly decreased during SP treatment. **d** Lung burst amplitude significantly increased during SP treatment. **e** Representative neurograms during baseline (*top*), SP (*middle*) and antagonist D (*bottom*) treatments. Data are mean ± SEM. *Asterisk* indicates a significant difference from all other groups and *number signs* indicate a significant difference from baseline ($n = 7$; $P < 0.05$)

NIH-PA Author Manuscript

NIH-PA Author Manuscript

NIH-PA Author Manuscript

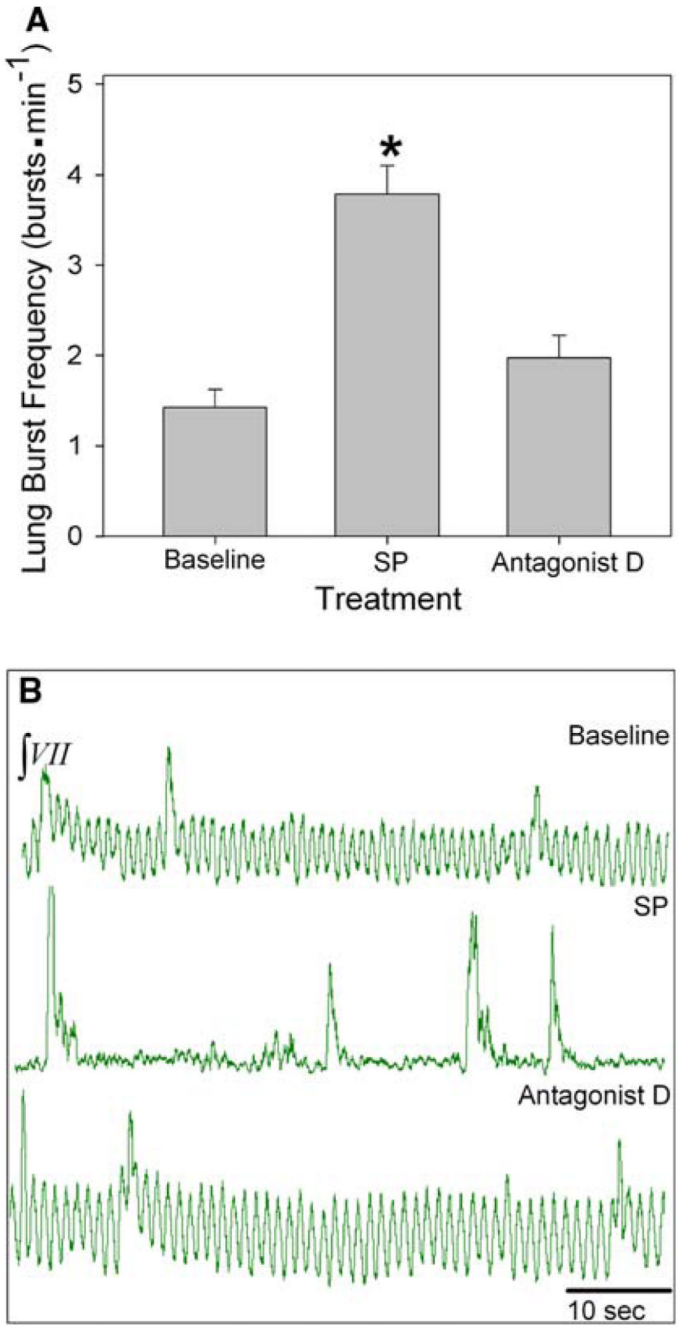

Fig. 3.

Role of NK1R in early-stage tadpole respiratory rhythm generation. **a** Lung burst frequency significantly increased during SP treatment. **b** Representative neurograms during baseline (*top*), SP (*middle*) and antagonist D (*bottom*) treatments. Data are mean ± SEM. *Asterisk* indicates a significant difference from all other groups ($n = 6$; $P < 0.05$)

NIH-PA Author Manuscript
NIH-PA Author Manuscript
NIH-PA Author Manuscript

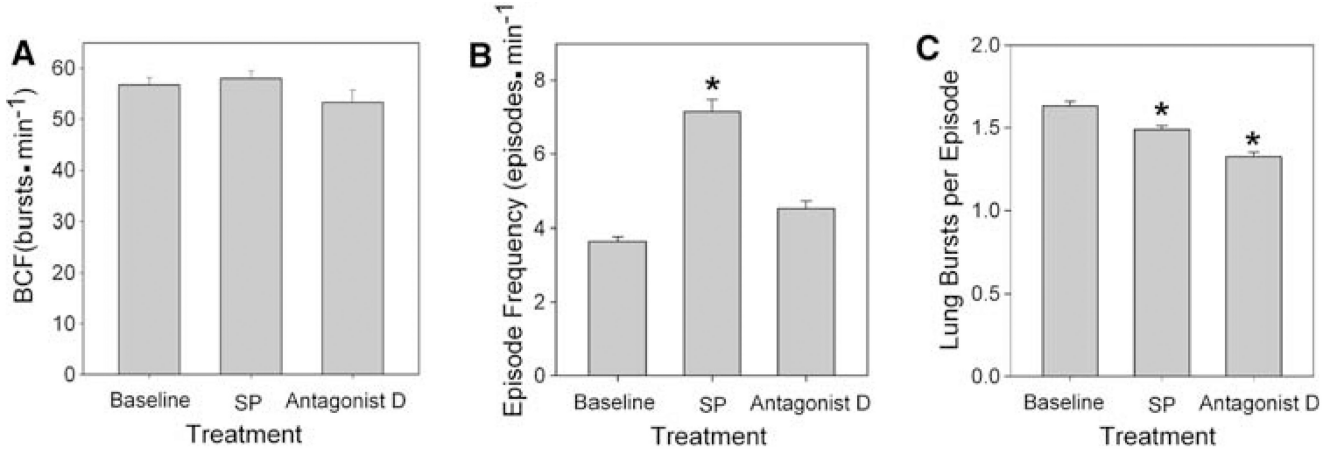

Fig. 4.

Role of NK1R in juvenile bullfrog respiratory episodic pattern generation. **a** Burst cycle frequency increased during SP treatment and decreased below baseline during antagonist D treatment. **b** SP significantly increased episode frequency and **c** significantly decreased the number of lung bursts per episode. Data are mean ± SEM. *Asterisk* indicates a significant difference from all other groups ($n = 7$, $P < 0.05$)

NIH-PA Author Manuscript

NIH-PA Author Manuscript

NIH-PA Author Manuscript

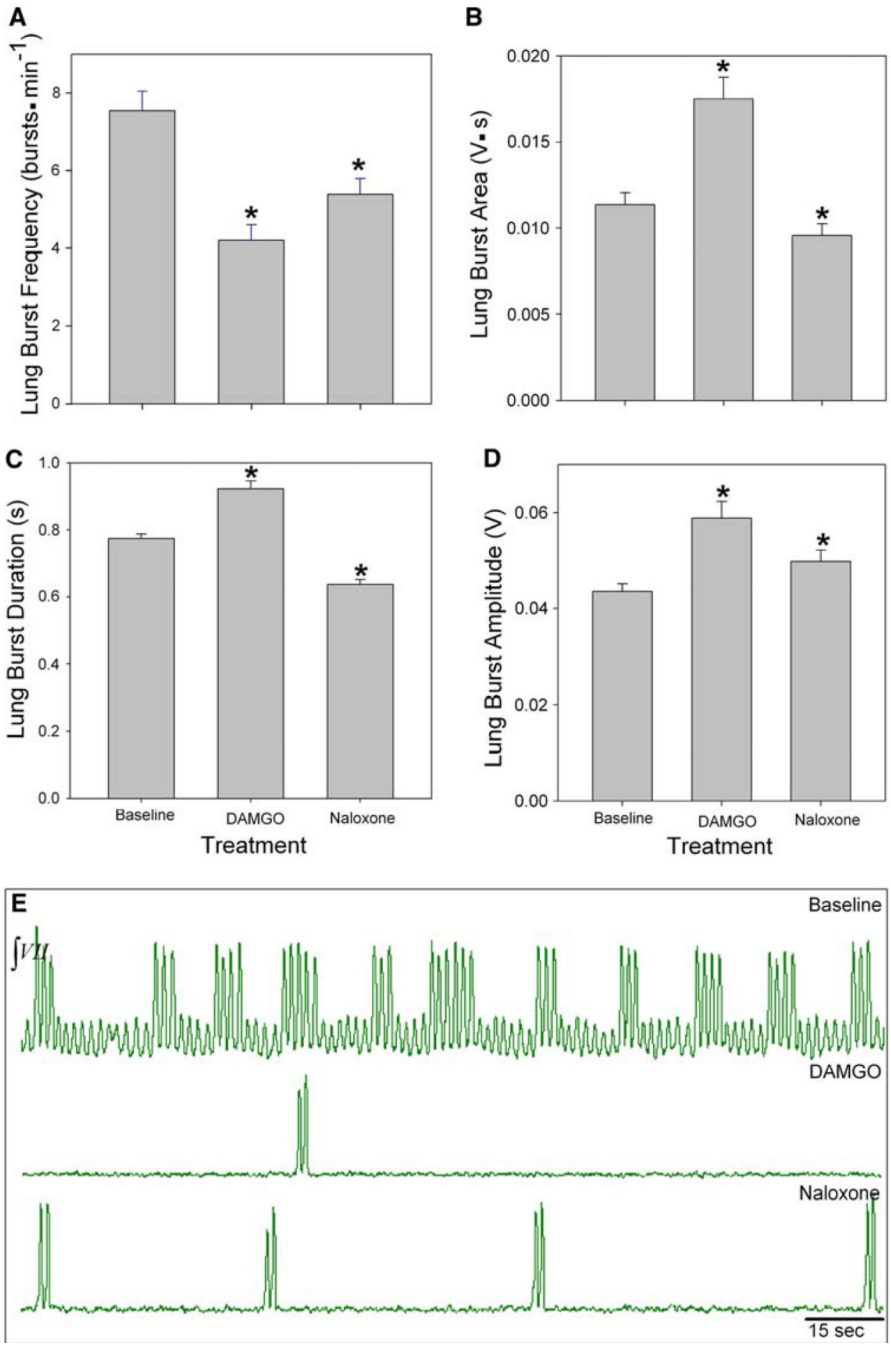

Fig. 5.

Role of μOR in juvenile bullfrog respiratory rhythm generation. **a** Lung burst frequency significantly decreased during DAMGO treatment. **b** Lung burst area **c** duration, and **d** amplitude significantly increased during DAMGO treatment. **e** Representative neurograms during baseline (*top*), DAMGO (*middle*), and naloxone (*bottom*) treatments. Data are mean ± SEM. *Asterisk* indicates a significant difference from all other groups ($n = 5$, $P < 0.05$)

NIH-PA Author Manuscript

NIH-PA Author Manuscript

NIH-PA Author Manuscript

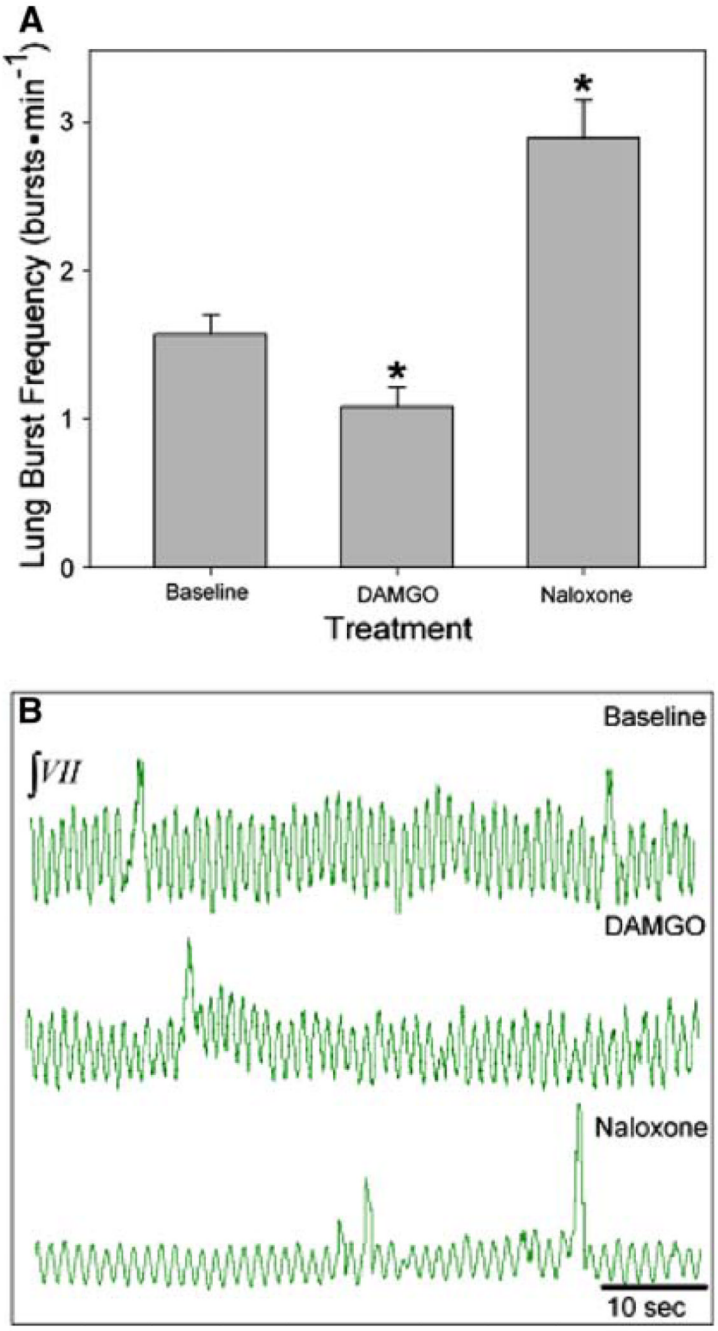

Fig. 6.

Role of μOR in early-stage tadpole respiratory rhythm generation. **a** Lung burst frequency significantly decreased during DAMGO treatment and increased above baseline during naloxone treatment. **b** Representative neurograms during baseline (*top*), DAMGO (*middle*), and naloxone (*bottom*) treatments. Data are mean ± SEM. *Asterisk* indicates a significant difference from all other groups ($n = 6$, $P < 0.05$)

NIH-PA Author Manuscript
NIH-PA Author Manuscript
NIH-PA Author Manuscript

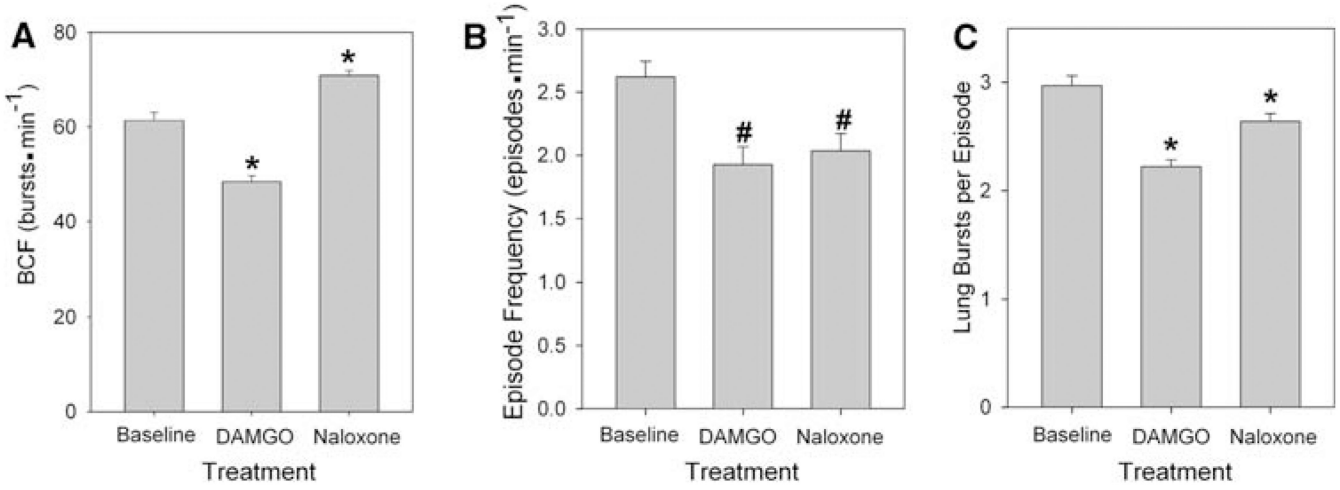

Fig. 7.

Role of μOR in juvenile bullfrog respiratory episodic pattern generation. **a** Burst cycle frequency, **b** episode frequency, and **c** lung bursts per episode significantly decreased during DAMGO treatment. *Asterisk* indicates a significant difference from all other groups and number signs indicate a significant difference from baseline ($n = 5$, $P < 0.05$)